DANISH METEOROLOGICAL INSTITUTE

SCIENTIFIC REPORT

97-2

Analysis of Tropospheric Ozone Measurements in Greenland

Contract No. EV5V-CT93-0318 (DG 12 DTEE)
DMI's contribution to CEC Final Report
Arctic Tropospheric Ozone Chemistry
ARCTOC

Alix Rasmussen
Sissi Kiilsholm
Jens Havskov Sørensen
Ib Steen Mikkelsen

DMI

COPENHAGEN 1997

ISSN-Nr. 0905-3263
ISBN-Nr. 87-7478-361-0

Contents

Analysis of Tropospheric Ozone Measurements in Greenland

A. Rasmussen, S. Kiilsholm, J. Havskov Sørensen and I. S. Mikkelsen

Danish Meteorological Institute (DMI)

Lyngbyvej 100, DK-2100 Copenhagen Ø, Denmark

1. Introduction/Summary

DMI initiated continuous measurements of surface ozone concentrations in Greenland during spring 1994 as a part of the EU-project ARCtic Tropospheric Ozone Chemistry (ARCTOC). The objectives are to investigate the mechanisms causing sudden arctic tropospheric ozone loss, spatial extent and possible consequences of the phenomenon.

In this report we will focus on the extent of the ozone loss phenomena and the physical (meteorological) environment of the phenomena. The chemical environment and possible mechanisms causing the ozone loss will not be discussed in detail partly because we do not have any measurements of relevant trace constituents (as BrO, ClO and IO) and partly because the ARCTOC measuring campaign in Ny-Aalesund, Svalbard, already has identified that the cause of the sudden tropospheric ozone loss mainly is due to bromine and chlorine catalysis with BrO as the most essential ingredient. The main outstanding problem is to determine the source, dispersion and lifetime of the relevant constituents.

The observation sites in Greenland are Thule, Søndre Strømfjord and Scoresbysund, cf. fig. 1 and fig. 10 in appendix. In addition to the continuous surface ozone measurements vertical profiles of ozone concentrations were measured at least weekly in Thule and Scoresbysund by ozone sondes. In Søndre Strømfjord only a few scattered ozone sondes measurements were taken.

In 1994 no definite periods with ozone depletion were recorded (here "depletion" is used when ozone concentrations are significantly below normal, but not necessarily zero). But there were strong indication of an episode in the start of the measurements in Thule around 13th April and analysis of ozone sonde data indicates an episode in mid March. Periods with low ozone concentrations were observed in May and June, especially in connection with fronts passing from west.

In 1995 and '96 several events of deep ozone depletion were recorded at Thule and Søndre Strømfjord connected with passing frontal systems (cold fronts) from west or northwest with rising pressure and falling temperature. At Scoresbysund minor episodes were observed both in 1995 and '96.

The major episodes could definitely be defined to cold air masses moving from the Arctic Ocean north of the Canadian Archipelago across Baffin Bay and Davis Strait and further crossing Greenland.

Analysis of backward trajectories calculated by DMI's 3-D transport model utilising meteorological data from the numerical weather prediction model DMI-HIRLAM (HIgh Resolution Limited Area Model) has been performed. Results from the study show that the air parcels with low ozone values at the receptor point generally have their origin in the northern Canadian Archipelago and in the Arctic Ocean.

2. Measurements

Surface ozone concentrations in Greenland have been observed by the Danish Meteorological Institute (DMI) in Thule from April 1994, in Scoresbysund from May 1994 and in Søndre Strømfjord from May 1995.

The monitor in Thule, cf. fig. 1, is located at the South Mountain 240 meters above sea level just south of the Thule Air base. In Scoresbysund the monitor is located near the top of a small local hill about 65 meters above sea level in connection with the telestation 500 meters east of the village. In Søndre Strømfjord the monitor is located 5 km southeast of the air base near the top of a small hill 320 meters over sea level. The instruments are photometric ozone analyzers, model 400 from Advanced Pollution Instrumentation. Data averaged over 10 minutes are automatically collected on a PC and sent to DMI either directly (ftp) or via diskette.

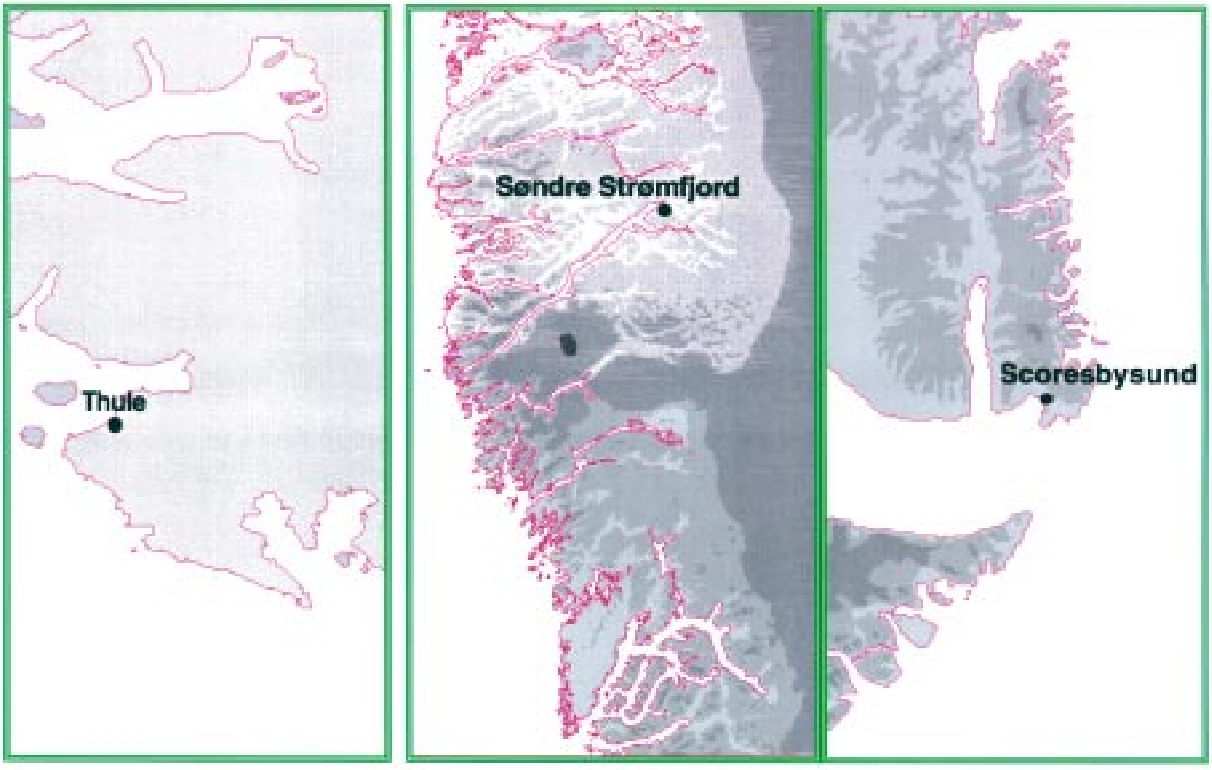

Fig. 1. Map showing the observation sites in Greenland measuring surface ozone concentrations. Thule (76°31'N, 68°50'W), Søndre Strømfjord (67° 00'N, 50° 48'W) and Scoresbysund (70° 29'N, 21° 58'W).

Fig. 2 shows the daily mean ozone concentrations in Thule, Scoresbysund and Søndre Strømfjord for the years 1994, 1995 and 1996. There is a clear seasonal variation with average values generally from 35-40 ppb, during the months June to August the values decrease to about 25 ppb.

In 1994 it seems that Thule experienced a depletion episode at the start of the measurements in April, while minor episodes were recorded in June. In Scoresbysund three minor episodes occurred in May and early June.

et al., in preparation for Tellus). Both episodes were clearly connected with a cold air mass moving from the northern Canadian Archipelago to Greenland. In Scoresbysund minor episodes were recorded in May and primo July.

In 1996 a major episode was recorded around 20 March. This episode was measured at all three stations, cf. appendix. A major similar episode was also recorded in Thule ultimo April.

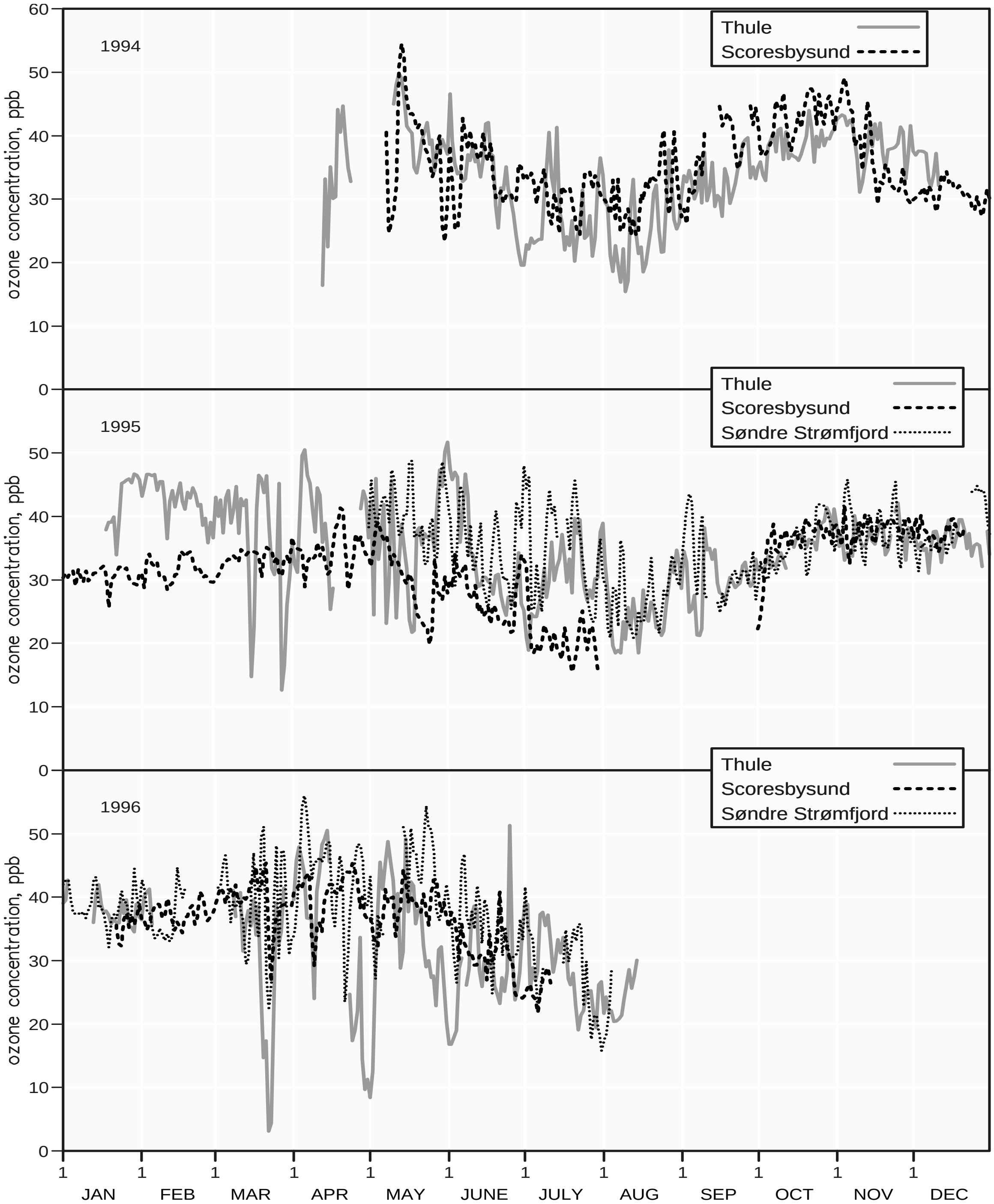

Fig. 2. Daily mean ozone concentrations (ppb) for Thule, Scoresbysund and Søndre Strømfjord for the years 1994, 1995 and 1996.

In fig. 3 a closer look is given for the episode in March 1996. The hourly mean ozone concentrations are until the 19th around 40 ppb, but in Thule the concentrations fall sharply to about 12 pbb during 4-5 hours. During the next two days the concentrations in Thule slowly increases to nearly 20 ppb, then suddenly falling to below 5 ppb during the 22nd. During the 24th to 25th the level in Thule increases to about 50 ppb. In Søndre Strømfjord the concentrations fall rather slowly during the 21st to about 16 ppb, while in Scoresbysund the concentrations fall sharply to 21 ppb during three hours on 22 March. Inspection of weather maps, cf. appendix, shows that the episode is connected with a cold air mass moving from the Arctic Ocean and northern Canadian Archipelago to east and southeast across Greenland.

An interesting feature on the figure is the very short lived low ozone episode observed both in Thule and Søndre Strømfjord 26th March. The episode occurred in connection with a cold air mass approaching from west-southwest (cf. appendix) with precipitation.

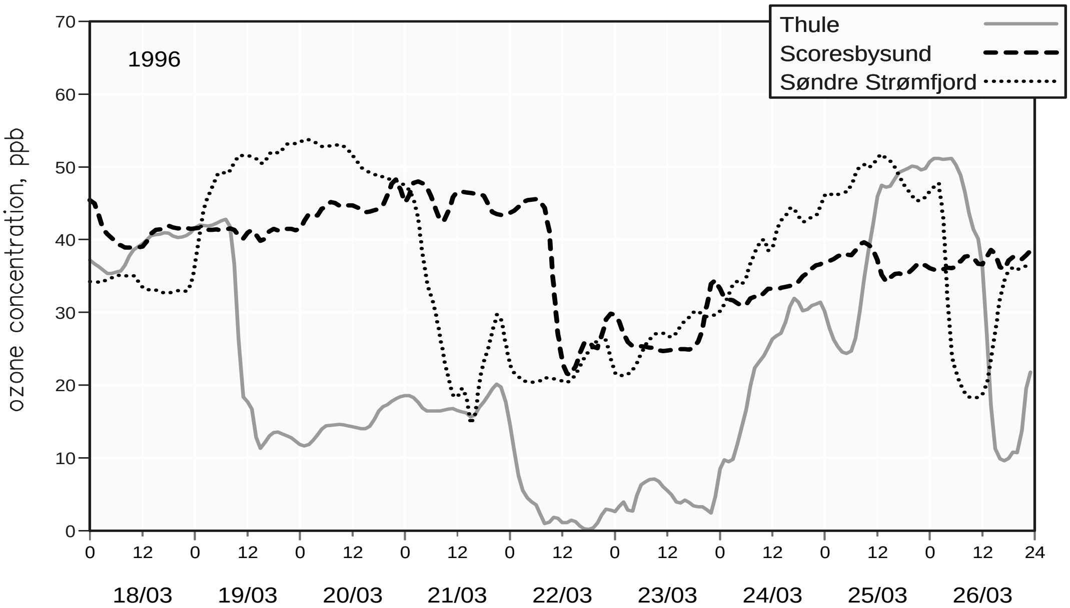

Fig. 3. Hourly mean ozone concentrations (ppb) for Thule, Scoresbysund and Søndre Strømfjord for the period 18th to 26th March 1996.

Fig. 4. shows time series of hourly ozone concentrations, pressure and temperature in Thule for the same period. The 19th the temperature drops from about -16^{o}C to about -30^{o}C and on the 22nd with the most intense ozone depletion the temperature falls to about -36^{o} C. The pressure only increases slightly in connection with the first sharp decrease in ozone on the 19th March, while the pressure rises to above 1035 hPa during the most intense depletion period. The wind shift is quite marked in connection with the front passing the 19th, while there is no windshift on the 21st. Note also that there is no wind shift for the short episode on 26 March, but a pronounced increase in wind velocity.

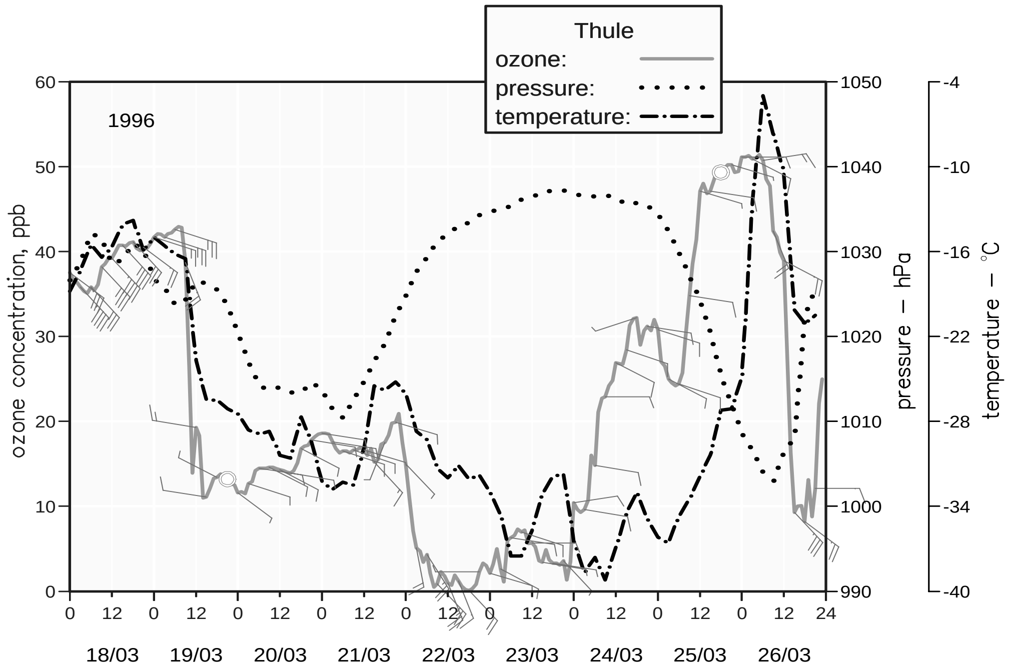

Fig. 4.: Time series of surface ozone concentrations (ppb), pressure (hPa), temperature (^oC) and wind at Thule for the period 18th to 26th March 1996. Meteorological parameters are taken from the synoptic station, 04202, at Thule Air Base.

In table 1 below, the correlation between ozone concentrations and some meteorological parameters are given. Generally the correlation coefficients are rather small, but especially for 1996 there is a significant positive correlation between temperature and ozone concentrations and anticorrelation between pressure and ozone concentrations. The correlation coefficients between wind velocity and ozone concentrations are very small, which is in accordance with the findings for data from Svalbard (Solberg et al, (1994))

	Temperature	Pressure	Wind-velocity	Wind-direction
Thu, 1995, 03	-0.07	-0.03	0.16	0.04
- - , 03-05	0.10	-0.17	0.14	-0.02
Thu, 1996, 03	0.52	-0.57	0.08	-016
- - , 03-05	0.25	-0.22	0.16	-0.05
Sco, 1995, 03	0.30	-0.12	0.17	0.02
- - , 03-05	-0.15	-0.06	0.07	0.02
Sco, 1996, 03	0.75	0.09	-0.18	0.00
- - , 03-05	0.26	0.02	-0.12	-0.05
SSt, 1996, 03	0.60	-0.29	0.18	0.10
- - , 03-05	0.44	-0.03	0.08	0.08

Table 1. Correlation coefficient between hourly mean surface ozone concentrations and the meteorological parameters: temperature, pressure, wind velocity and wind direction. Calculated for the month March (03) and March to May (03-05) for 1995 and ´96. Meteorological parameters are from synoptic stations nearby.

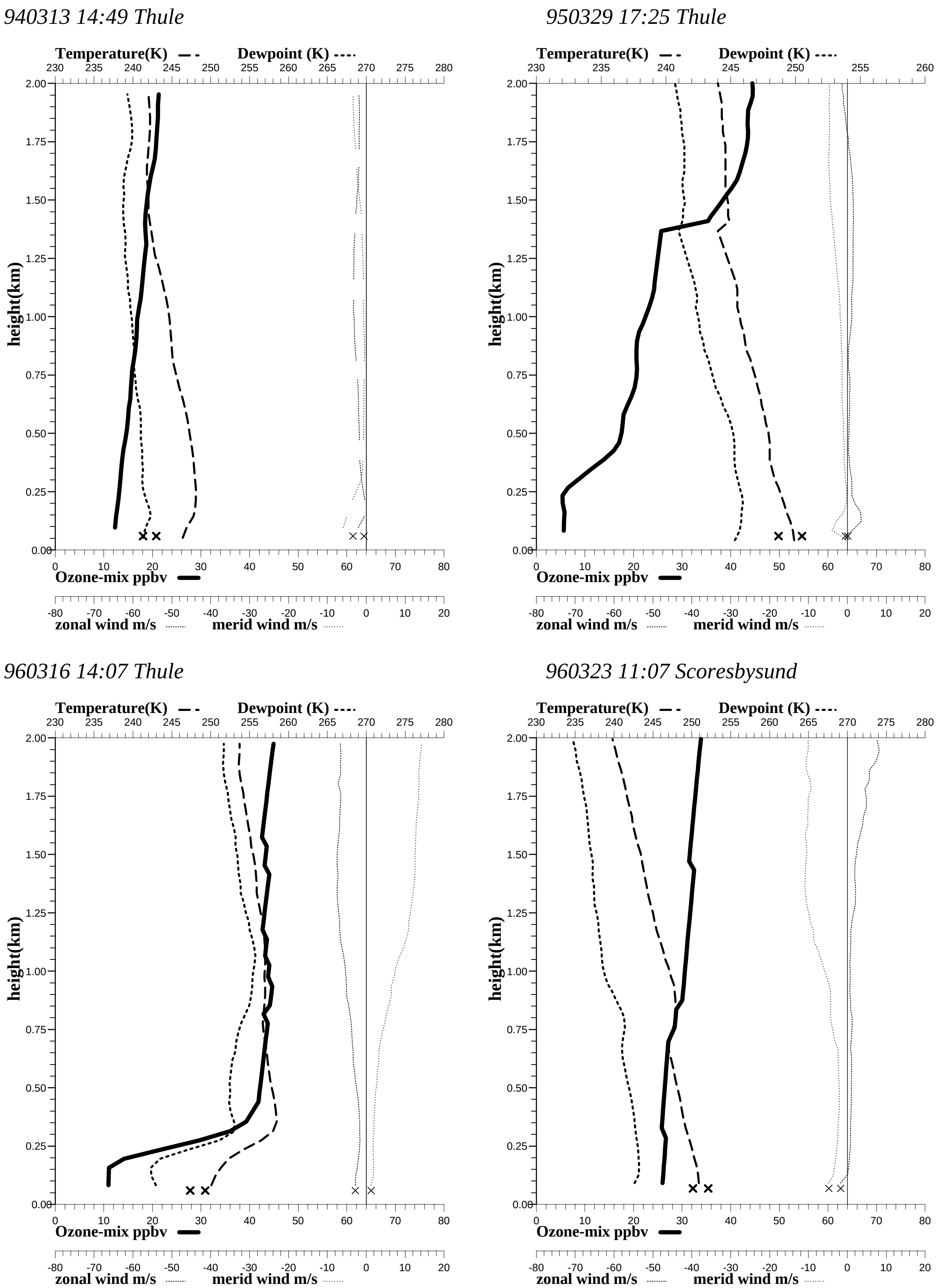

Fig. 5.: Ozone soundings from Thule for 13.03.94 14:49 UTC, 29.03.95 17:26 UTC and 16.03.96 14:07 and from Scoresbysund from 23.03.96 11:07 UTC. Profiles of temperature, dewpoint temperature, zonal, and meridional wind velocity are shown.

In fig. 5 a sample of 3 ozone soundings from Thule and 1 sounding from Scoresbysund is shown. For the profile at Thule from 13 March 1994 the concentration are low near the surface, about 12 ppb, and only slowly increasing to about 20 ppb at 2 km. The profile from 29 March 1995 is quite different with very low concentrations, app. 6 ppb, in a well mixed layer up to about 250 meters. Up to about 400 meters the concentration increases rather sharply to just below 20 ppb, slowly increasing to about 26 ppb up to 1350 meters, then sharply increasing to above 40 ppb. The profile indicates downward flux of ozone from a entrainment zone at 250-400 meters. Probably the ozone destroying process is still active with positive concentrations of BrO - in the ARCTOC measuring campaign at Ny-Aalesund it was found that non-zero concentrations of ozone and BrO could co-exist for several days, while the chemistry with the measured level of BrO would dictate ozone destroying during short time.

The profile from 16 March 1996 also shows a well mixed layer from ground up to about 175 meters with concentration just above 10 ppb, sharply increasing to above 40 ppb at 300 meters.

The profile from Scoresbysund, 23 March 1996, is from the already mentioned episode affecting all three monitoring stations, cf. fig. 3. It appears that the ozone in the whole column up to 2 km is fairly well mixed with concentrations slowly increasing from app. 26 ppb to app. 35 ppb at 2 km. The air mass trajectory (cf. next section) is from the Arctic Ocean just north of the Canadian monitoring station Alert and along the northeastern coast of Greenland. The original air mass has presumably (cf. appendix) been exposed to deep ozone depletion near ground, but on the long way from the Arctic Ocean strong vertical mixing especially along the complex north-eastern coastal area of Greenland will cause the profile observed.

Inspection of many ozone profiles from Scoresbysund all show fairly well mixed ozone up to at least 2 km. This can perhaps lead to the conclusion that the ozone destroying mechanism hardly can be effective along the coast of northeastern Greenland, or alternatively the vertical mixing near the monitoring station must be very strong (otherwise we should observe profiles with low concentrations near surface, as in Thule)

3. Trajectory analysis

3.1 Description of the transport model

The general features of DMI's 3-D transport model are described by Sørensen (1993). The trajectories are calculated by a standard iteration method (Kålberg (1984)) with a prescribed tolerance. The advection time step used is set to 15 minutes. The model can utilise data from the different versions of DMI-HIRLAM (see below) and from the global model at the European Centre for Medium-Range Weather Forecast (ECMWF).

The model is used for many purposes, e.g. as a part of the Danish Emergency Response Model for the Atmosphere (DERMA, Sørensen and Rasmussen (1995)) and in the Danish Atmospheric Chemistry Forecasting System (DACFOS, Jensen et. al (1996)). It is also used by the duty forecaster for estimating the movement of weather systems as well as in studies of the intrusion of stratospheric ozone into the troposphere.

Parameters along the trajectory can be seen in table 2 below. The height of the boundary layer is calculated within the transport model from DMI-HIRLAM vertical profiles of temperature, wind and humidity using a bulk Richardson number method.

Table 2. Present parameters along 3-D trajectories based on DMI-HIRLAM	
at trajectory level	*at surface and 10-meter*
• Coordinates • Orography • Height above ground (of trajectory) • Horizontal wind (u,v) • Temperature • Relative humidity	• 10-meter horizontal wind (u,v) • Surface temperature • Precipitation intensity • Total cloud cover • Surface pressure • Surface fluxes of heat • Surface fluxes of momentum • Height of the mixing layer

3.2 The HIRLAM model

The HIgh Resolution Limited Area Model (HIRLAM) (Källén (1996)) is a primitive-equation Numerical Weather Prediction (NWP) model. The horizontal grid is a regular spatially staggered latitude/longitude grid in a rotated spherical projection. The vertical coordinate is a terrain-following hybrid co-ordinate (Simmons and Burridge (1981)) which near the surface is identical with the sigma coordinate (sigma $=p/p_{surface}$), and approaches the pressure p with increasing height.

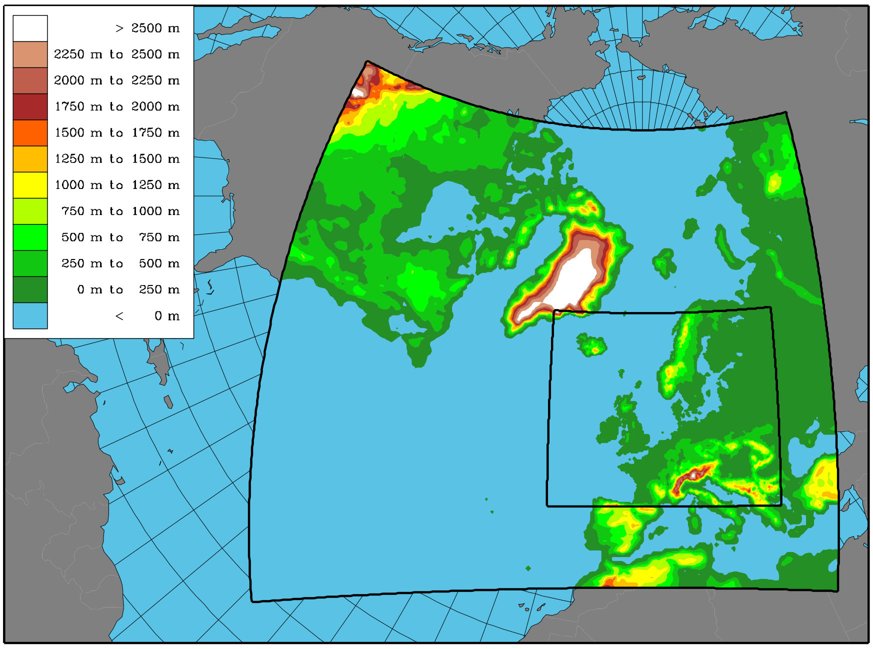

Fig. 6. The two areas used p.t. for DMI-HIRLAM. The inner area (Europe) is nested with the outer area (Greenland). The boundary fields for the large-area version (G) are obtained from the European Centre for Medium-Range Weather Forecast (ECMWF). The horizontal resolution is 0.42 deg. (46 km) for G and 0.21 deg. (23 km) for E.

The DMI-HIRLAM model (Hansen Sass (1994)) which is operational at the Danish Meteorological Institute (DMI), is run on two different limited areas. The Greenland (G) and Europe (E) models have the same vertical resolution (31 hybrid levels). The HIRLAM forecasting system consists of pre-processing, analysis, initialisation, forecast, post-processing and verification. Both model versions are run with their own 6-hourly data-assimilation cycle.

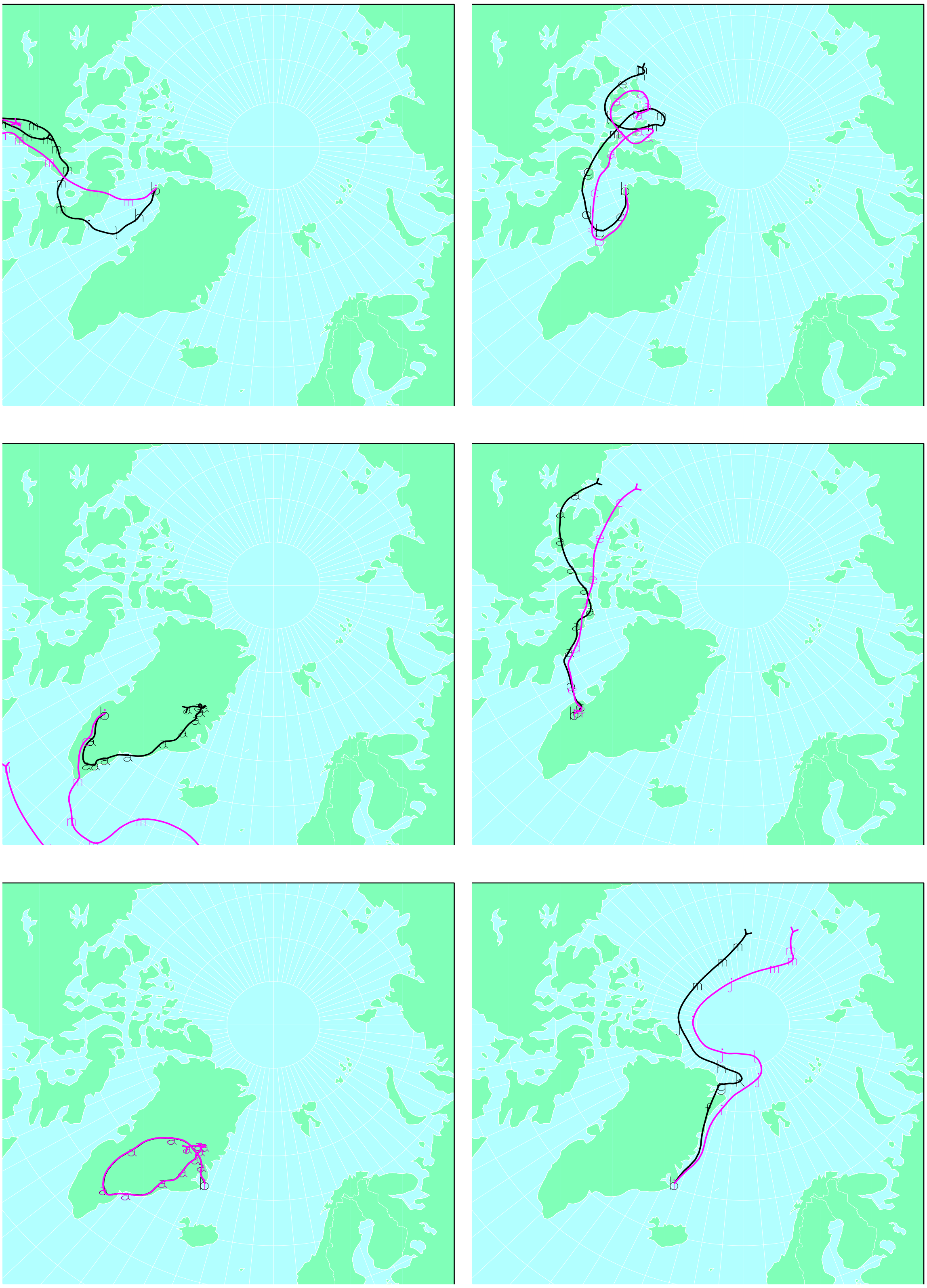

Fig. 7.: Trajectories for Thule, Søndre Strømfjord and Scoresbysund. At left from 19th March 00 UTC, 1996, and at right from 23 March, 00 UTC, 1996. The letters indicate the height of the trajectory relative to the ABL-height at the receptor point. Black trajectories arriving near ground and red/pink at the top of the ABL at the receptor point. Marks for every 12 hour.

3.3 Sector analysis

In fig. 7 an ensemble of (typical) trajectories for Thule, Søndre Strømfjord and Scoresbysund for 19 March 1996 (left side of the figure) and 23 March 1996 is shown. The two dates correspond to a non-depletion and a depletion episode respectively (cf. fig. 3). The two trajectories presented for each station differ in the arrival height at receptor point, respectively arriving at height 0.1 and 0.9 of the calculated ABL-height at the receptor point (cf. section 3.1). The length of the trajectories correspond to 5-6 days (provided they remain within the G-HIRLAM area) and time resolution of the trajectory data is 15 minutes.

A sector analysis of trajectories for the period March to May 1996 has been performed for Thule, Søndre Strømfjord and Scoresbysund. The analysis is based on a set of 4 trajectories each day (00 UTC, 06 UTC ..), each set consisting of five backward trajectories arriving at the receptor point (e.g. Thule) at equidistant heights between the ground and the top of the boundary layer.

In fig. 8.a-b a result of the sector analysis of the 72-hour backward trajectories for Thule for the period March to May 1996 is presented. The main part of the trajectories have their origin in the sector S - SE, but for the case of low ozone concentrations (<10 and <20 ppb) the largest number of trajectories come from the western sector.

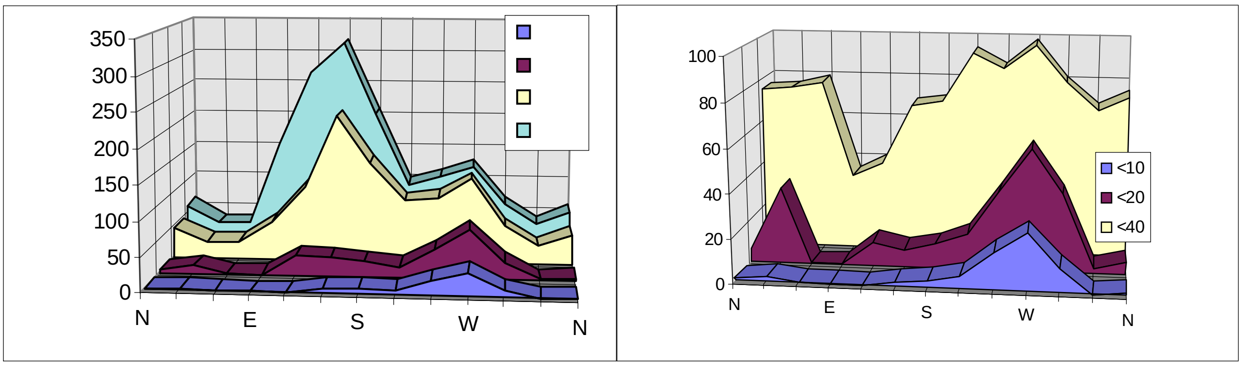

Fig. 8.a-b Sector analysis of 72 hour back-trajectories for Thule for the period March to April 1996. To left number of trajectories pr. sector (30. degrees) for different ozone concentrations at receptor point. To right percent of total number in sector.

In fig. 9.a-b the start-positions of back trajectories, respectively 72 hours and 96 hours long, for Thule for the period March to May 1996 are marked by a symbol dependent on the 6-hour mean ozone concentration at the receptor point in Thule. A * is used for observed ozone concentrations below 10 ppb, + for conc. between 10 and 20 ppb and above 20 ppb by a dot. It is clear from the figure that the main source region of low ozone concentrations going 72 hours back (fig. 9.a) is from the northern Canadian Archipelago. Going 96 hours back the conclusion is the same, but a number of low episodes have now their origin in the Polar Basin. Going further back (120 hour and 144 hours, not presented) gives a similar picture. It should be noted that very few trajectories have their origin in the area around Alert, where depletion episodes are more common than in Thule.

For Scoresbysund (not shown) the low ozone episodes (below 20 ppb) have their origin in the North Polar Basin. For Søndre Strømfjord the results are not so simple; the major part of the low ozone episodes (below 20 ppb) have their origin in the Canadian Archipelago, but some episodes have their origin around Hudson Bay and other from the area southwest of Greenland.

72 hours

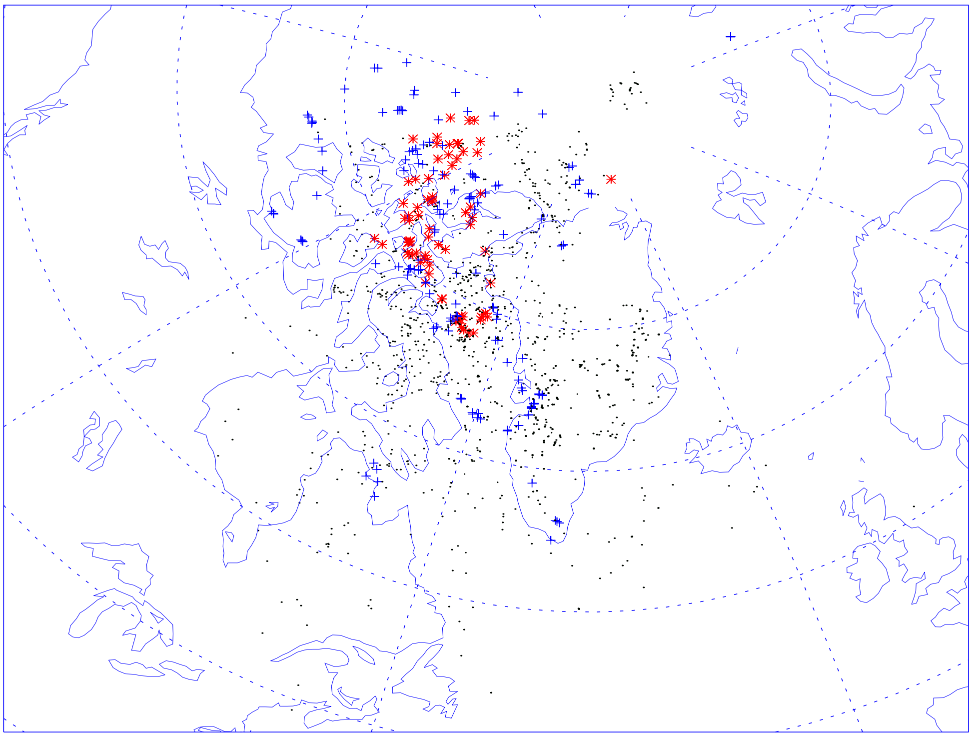

96 hours

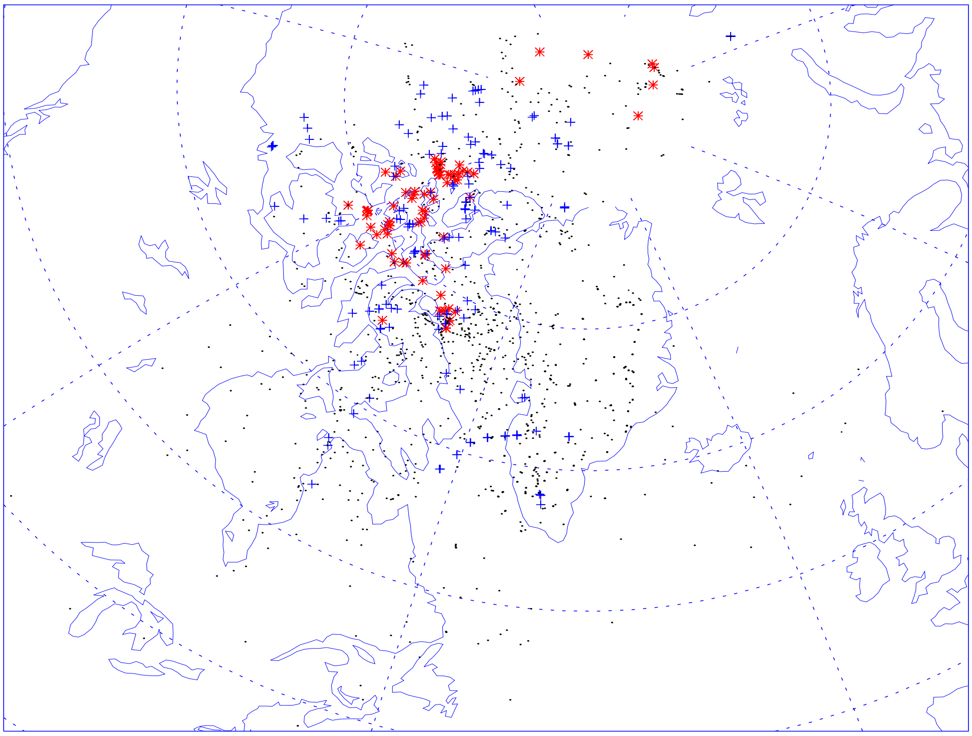

*Fig. 9.a-b Analysis of backward trajectories from Thule for the period March to May 1996, showing positions 72 hours (a,upper) and 96 hours (b, lower) respectively before arriving at Thule. Positions are marked by * for observed ozone concentrations below 10 ppb, by + for conc. between 10 and 20 ppb and otherwise by a dot. Ozone concentrations are 6-hour averages.*

4. Conclusion

The ozone measurements in Greenland have established the fact that the phenomenon of sudden arctic tropospheric ozone loss also appears in Greenland. It is most pronounced at the west-coast of Greenland and generally confined to the period from March to May. Spatially the phenomenon is very extended as a whole air mass from Thule to Søndre Strømfjord is seen to be affected by the phenomenon.

The major episodes could definitely be defined to cold air masses moving from the Arctic Ocean north of the Canadian Archipelago across Baffin Bay and Davis Strait and further crossing Greenland. Analysis of backward trajectories calculated by DMI's 3-D transport model utilising meteorological data from the numerical weather prediction model DMI-HIRLAM (High Resolution Limited Area Model) support this finding.

The chemical mechanisms causing the ozone loss has already been identified to be mainly due to bromine and chlorine catalysis with BrO as the most essential ingredient (Bottenheim et al., 1990, and ARCTOC measuring campaign in Ny-Aalesund), but still many outstanding problems are remaining, especially determination of the source, dispersion and lifetime of the relevant chemical constituents.

5. References

Bottenheim, J. W., Barrie, L.A, Atlas, E., Heidt, L.E., Niki, H., Rasmussen, R.A. and P.B. Shepson, 1990. 'Depletion of lower tropospheric ozone during Arctic Spring: The Polar Sunrise Experiment 1988.' J. Geophys. Res.,95D, 18,555-18,568

Barrie, L.A., J.W. Bottenheim and W.R. Hart, 1994. 'Polar Sunrise Experiment 1992 (PSE 1992): Preface', J. Geophys. Res., 99D12, 25,313-25,314

Solberg, S., O. Hermansen, E. Joranger, N., F. Stordal and Ø. Hov, 1994. 'Tropospheric ozone depletion in the Arctic during spring', NILU OR 27/94, ISBN 82-425-0575-6

Simmons, A.J. and D.M. Burridge, 1981. 'An energy and angular momentum conserving vertical finite-difference scheme and hybrid vertical coordinates.' Mon. Wea. Rev. 109, 758-766

Kållberg, P., 1984. 'Air parcel trajectories from analyzed or forecast windfields.' In *Workshop on simplified models for short-range forecasting on the mesoscale.* SMHI R & D notes **37**

Sørensen, J.H., 1993. 'Operational Dispersion Program, Version 1, Documentation Manual', DMI Technical Report 93-5, ISSN 0906-897X

Sørensen, J. H. and A. Rasmussen, 1995. 'Calculations Performed by the Danish Meteorological Institute', in: Report of the Nordic Dispersion/Trajectory Model Comparison with the ETEX-1 Fullscale Experiment, Eds: U. Tveten and T. Mikkelsen Risø-R-847(EN), NKS EKO-4(95)1, ISBN 87-550-2118-2, ISSN 0106-2840

Jensen, M.H., A. Rasmussen, H. Svensmark and J. Havskov Sørensen, 1996. 'Danish Atmospheric Chemistry Forecasting System (DACFOS)', DMI Technical Report 96-3, ISSN 0906-897X

Sass, B. H., 1994. 'The DMI Operational HIRLAM Forecasting System, Version 2.3.' DMI Technical Report 94-8

Källen, E. (Ed.), 'HIRLAM documentation manual, System 2.5.' *Available from SMHI* (1996)

APPENDIX

Ozone depletion episode in March 1996

The three surface ozone monitoring stations in Greenland (Thule, Søndre Strømfjord and Scoresbysund) registrated the episode from 19th to 24th March 1996, cf. fig. 3. The episode started in Thule 19. March 1996 at 09 UTC, in Søndre Strømfjord at 21. March 03 UTC and in Scoresbysund at 22. March 09 UTC. The episode was most pronounced in Thule.

***Selected weather maps from DMI-HIRLAM of msl-pressure and 925 hPa temperature and cross-sections of temperature and potential temperature*.**

Comments:

Fig. 11.a: 19.03.96 00 UTC a low pressure area and cold arctic air is situated over the north-western parts of the Canadian Archipelago and over the Arctic Ocean just north of the Archipelagos. The cold air is reaching Thule few hours later with a marked drop in the ozone concentration.

Fig. 11.b: 21.03.96 12 UTC the cold air has just reached Søndre Strømfjord causing a drop in the ozone concentration, while Thule experienced a minor local rise in the temperature (cf. also Fig. 4.).

Fig. 12.a: 23.03.96. 12 UTC the cold air has also reached Scoresbysund accompanied with a marked fall in the ozone levels. Notice that very cold air is situated over Thule experiencing deep ozone depletion.

Fig. 12.b: 25.03.96 12 UTC the cold air has crossed Greenland on its way further to east-southeast and some days later causing a "low ozone episode" in Denmark. Notice the cold air over Baffin Island moving east-northeast causing a short drop in the ozone levels the next day both in Thule and Scoresbysund.

Fig. 13.: The observed temperature profile at the radiosonde station Egedesminde (04220) on 19.03.96 11 UTC and 21.03.96 11 UTC, i.e. respectively before and after the start of the episode. The temperature fall is very marked from about $0^{o}C$ to about $-25^{o}C$. Notice also the shift in wind-direction from southeast-south to west.

Fig. 14.a-b: 18.03.96 12 UTC. Notice the well mixed cold air up to about 750 hPa, west of Ellesmere Island. All three monitoring stations are well within the warm air mass.

Fig. 15.a-b: 20.03.96 12 UTC. A cold tongue of air has reached Thule accompanied with ozone depletion, while Søndre Strømfjord and Scoresbysund still are in the warm air mass with normal ozone level.

Fig. 16.a-b: 23.03.96. 12 UTC. The cold air mass has reached all the three stations causing ozone depletion (cf. above). Notice the very cold air over Thule simultaneously with deep ozone depletion.

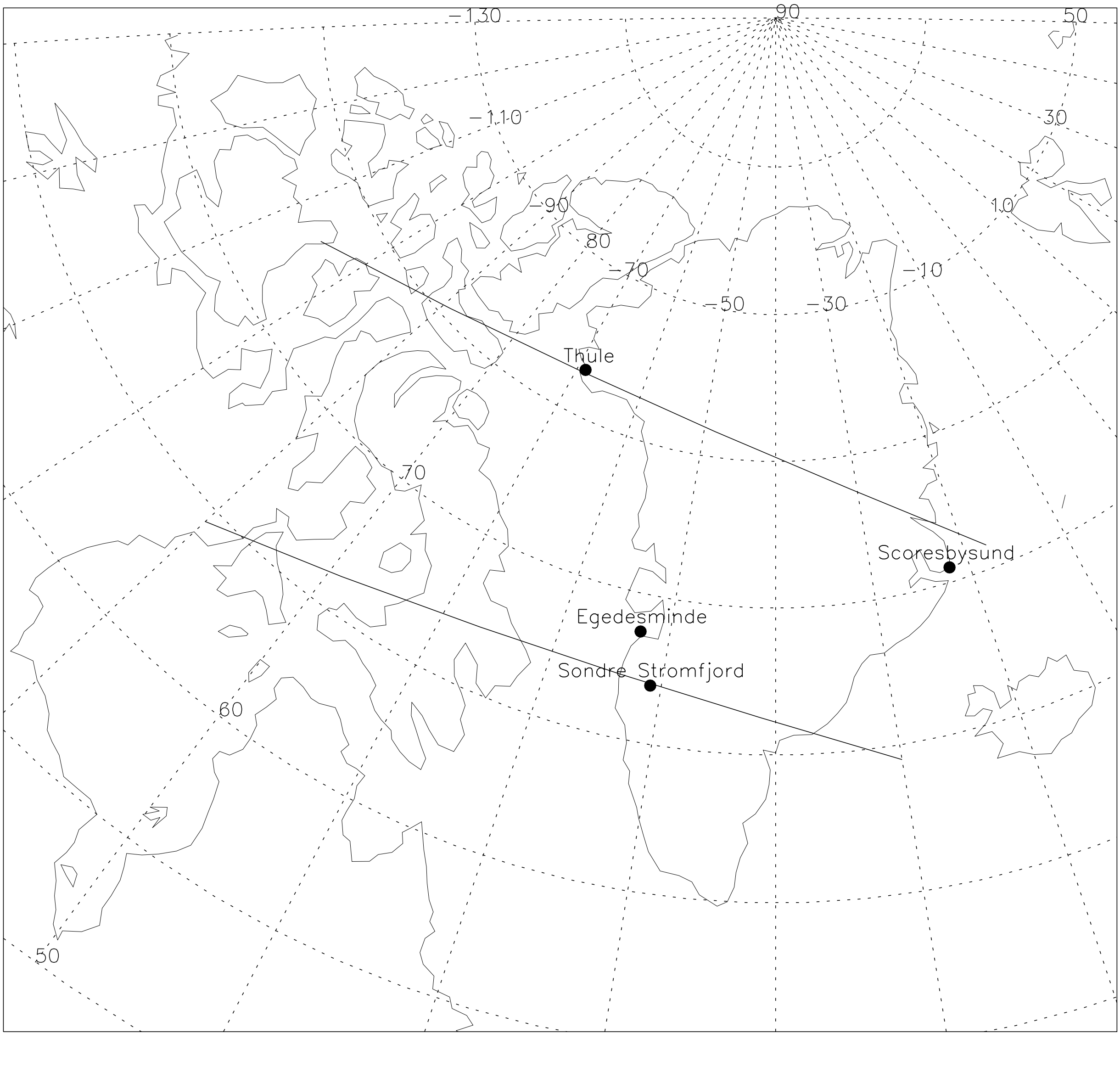

Fig. 10.: Map showing the ozone measuring sites in Thule, Søndre Strømfjord and Scoresbysund. and the radiosonde station at Egedesminde. The two cross sections lines, A (Thule and Scoresbysund) and B (Søndre Strømfjord), are also marked.

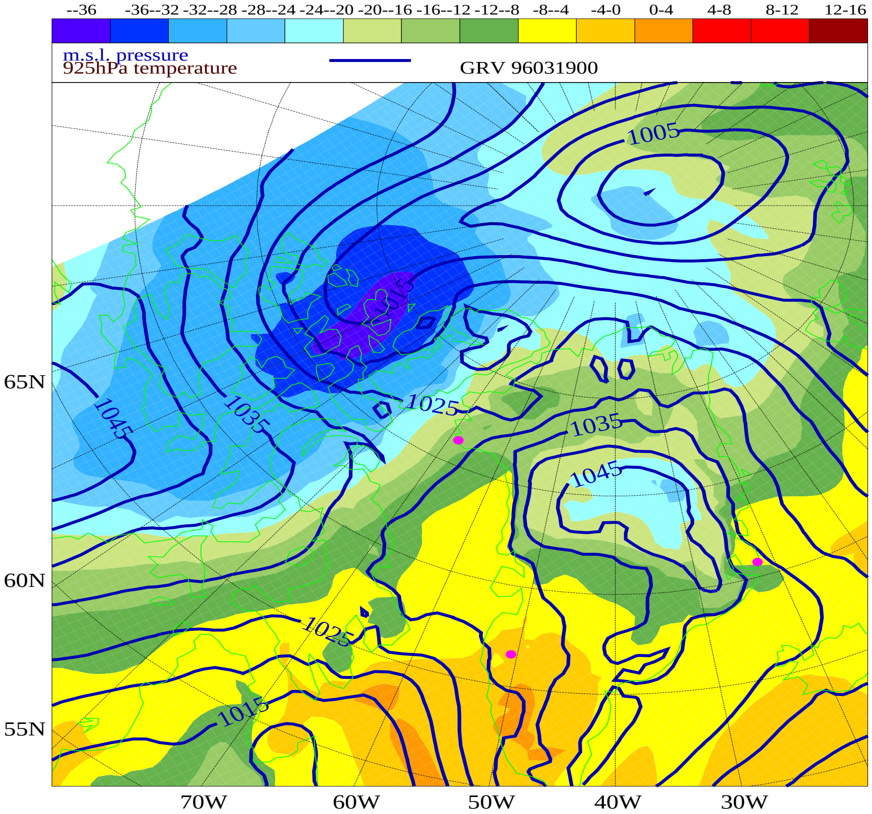

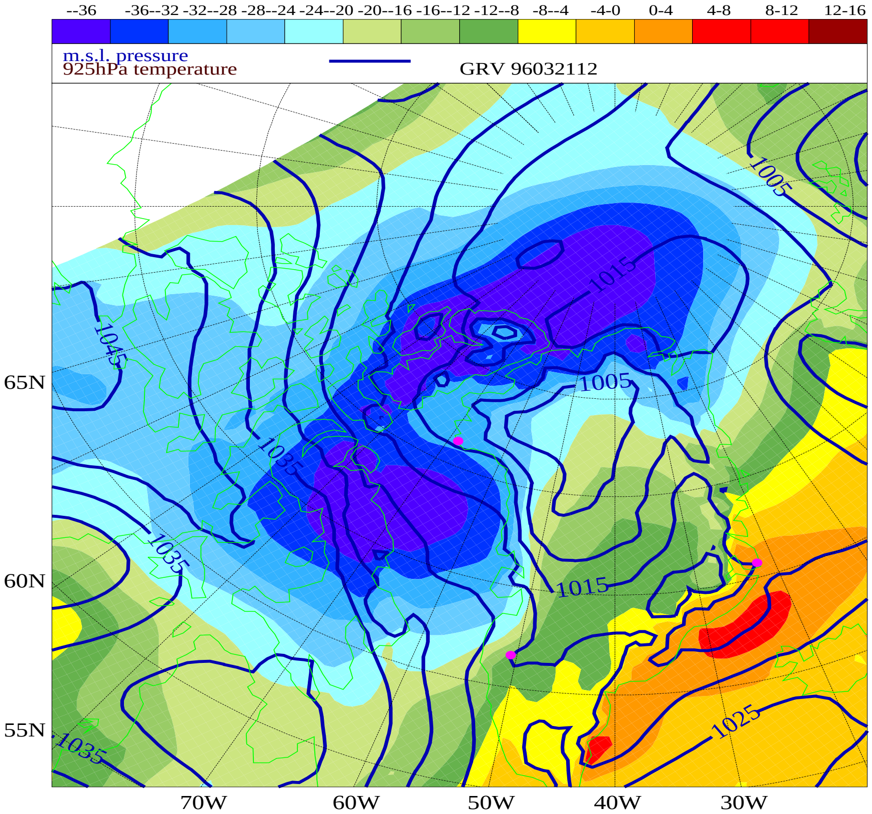

Fig. 11.a-b: DMI-HIRLAM map of msl-pressure and 925 hPa temperature respectively for 19.03.96 00 UTC and 21.03.96 12 UTC.

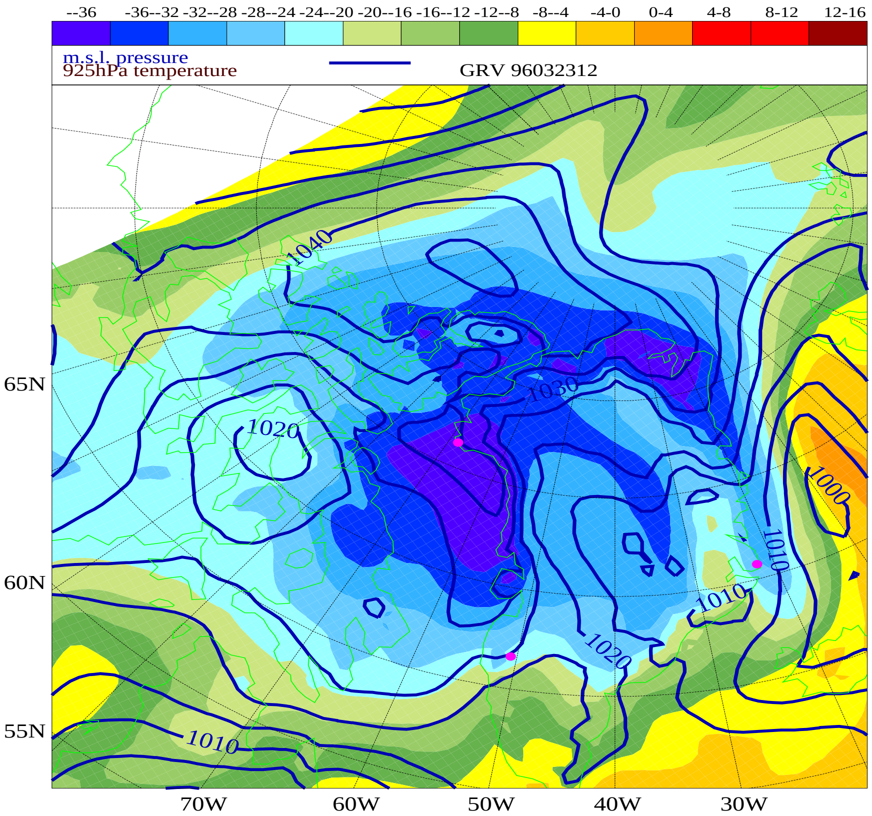

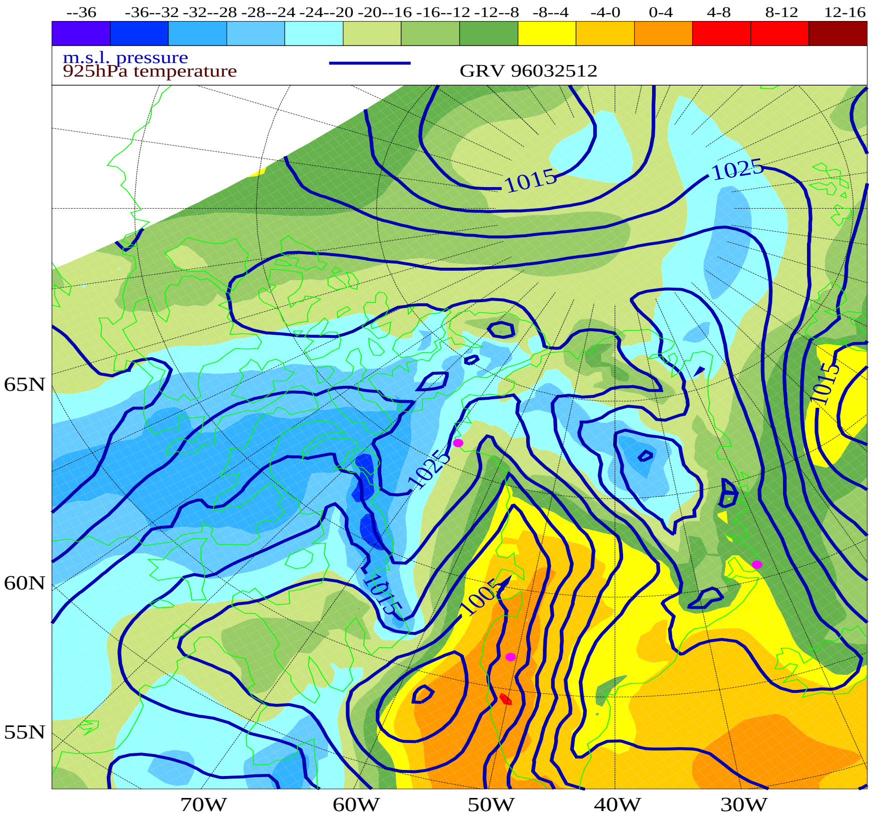

Fig. 12.a-b: Same as Fig. 10, but for 23.03.96 12 UTC and 25.03.96 12 UTC.

Egedesminde 960319 11 UTC

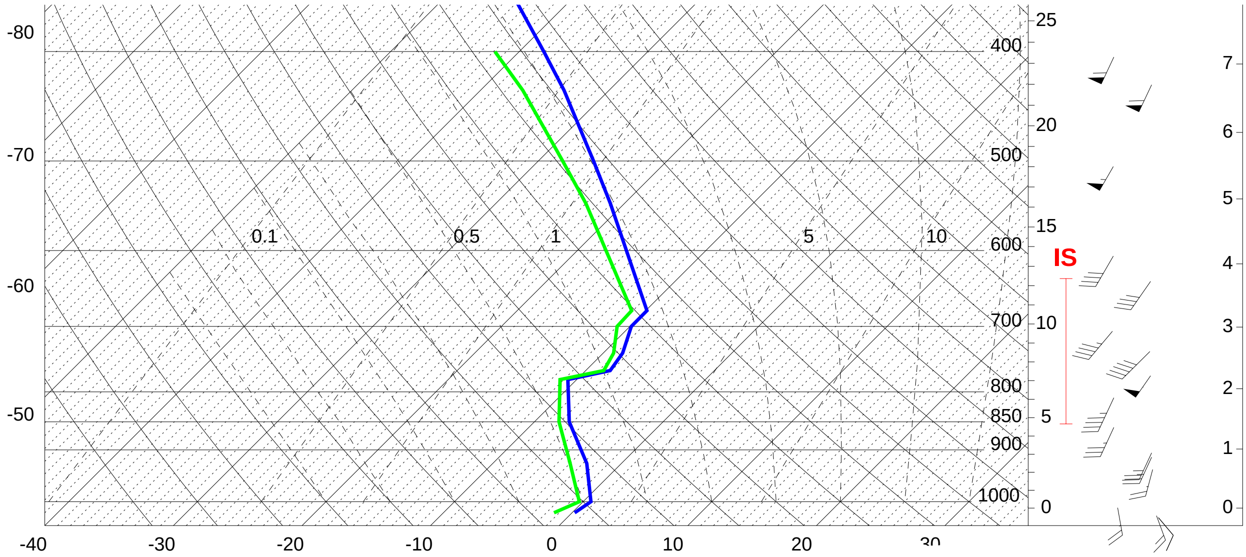

Egedesminde 960321 11 UTC

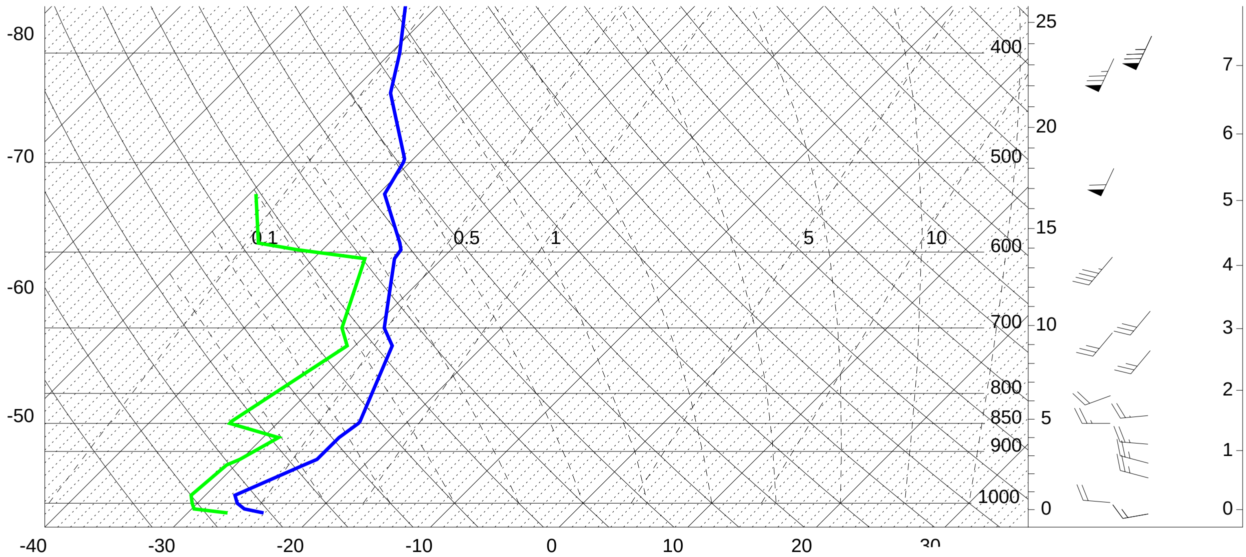

Fig. 13.a-b: Radio sounding from Egedesminde from respectively 19.03.96 11 UTC and 21.03.96 11 UTC

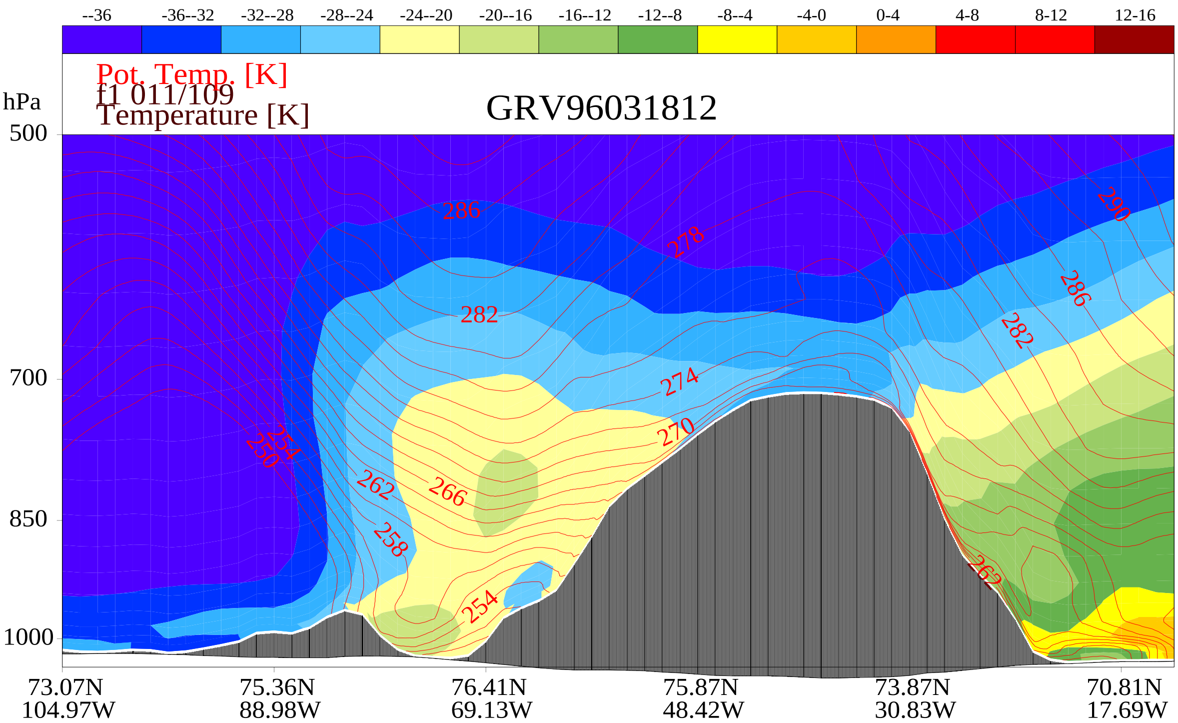

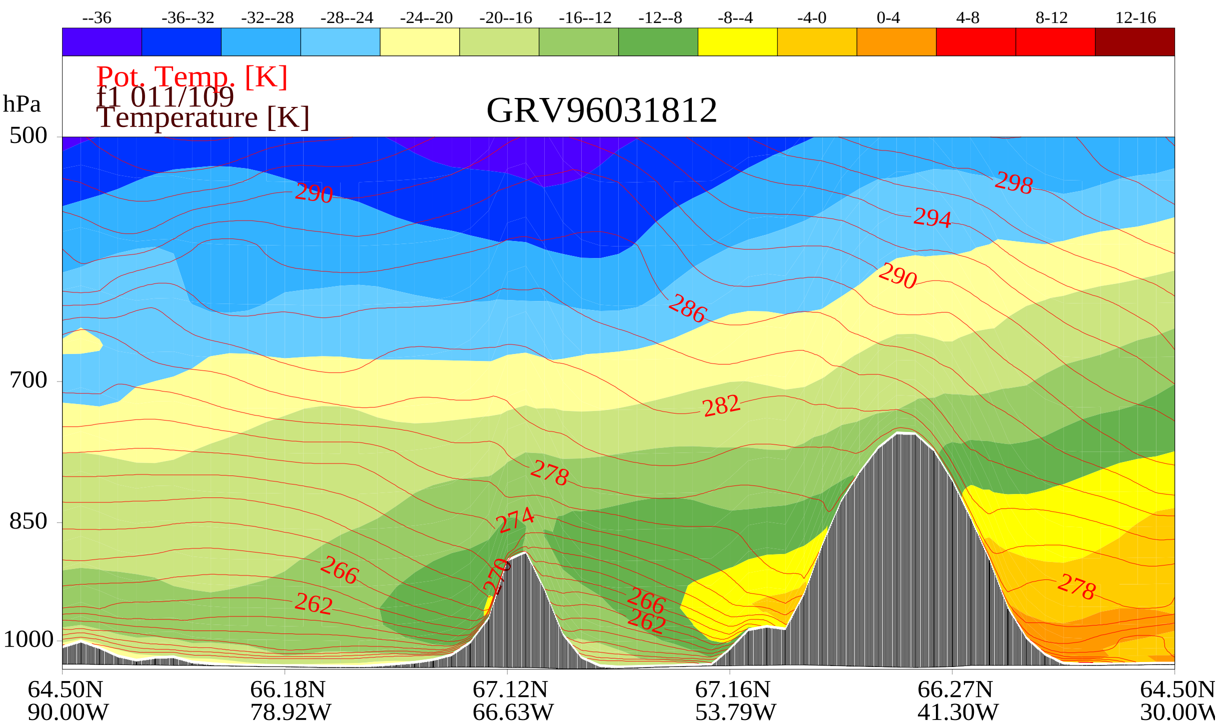

Fig. 14.a-b: DMI-HIRLAM cross section of temperature and potential temperature for the lines A (Thule and Scoresbysund) and B (Søndre Strømfjord). Date 18.03.96 12 UTC.

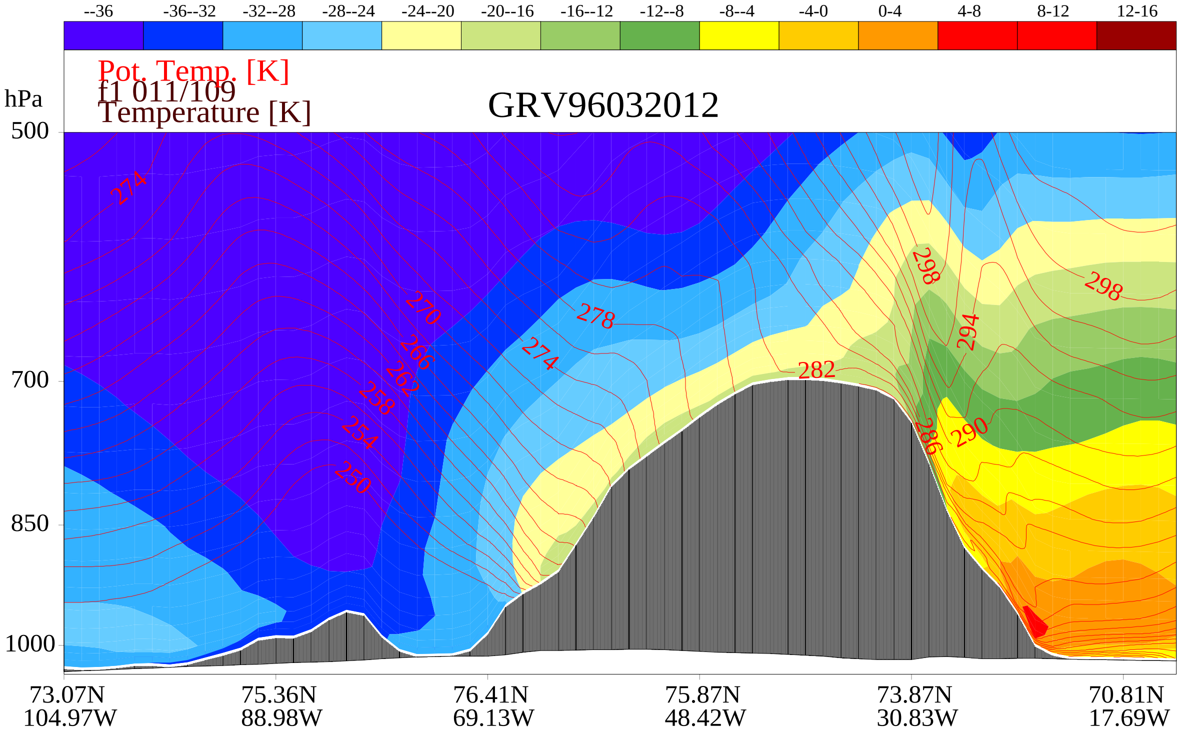

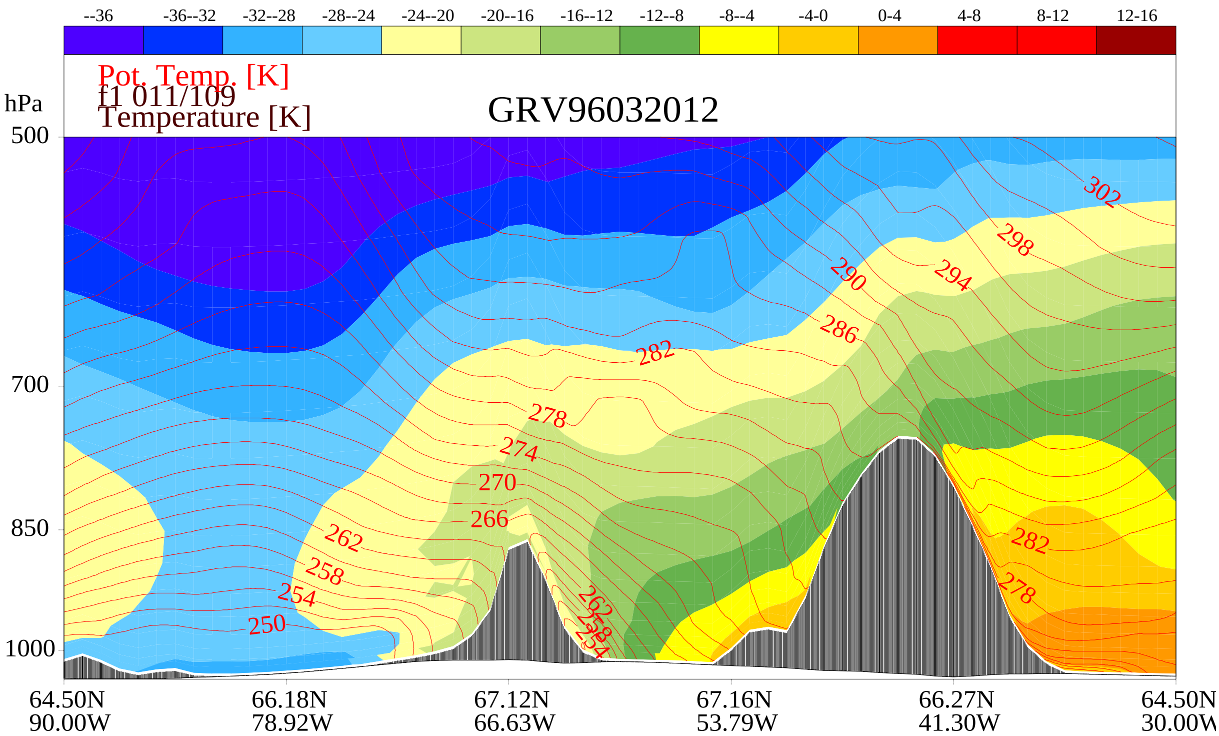

Fig. 15.a-b: Same as Fig. 13, but for the date 20.03.96 12 UTC.

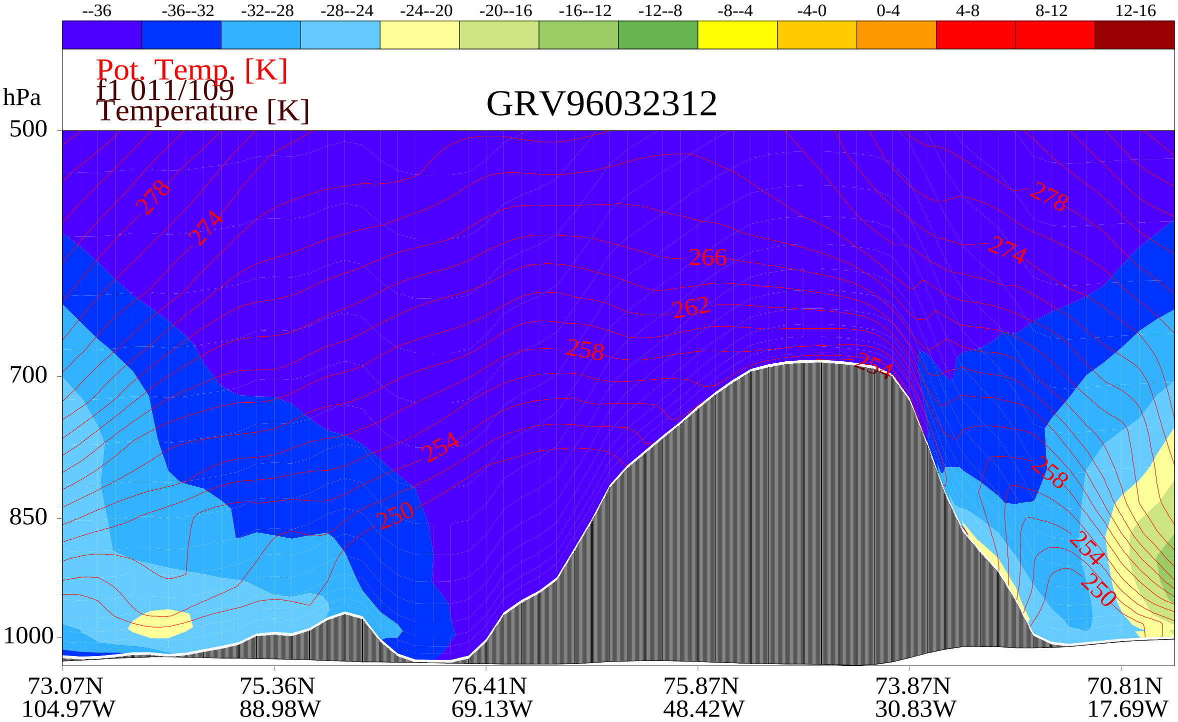

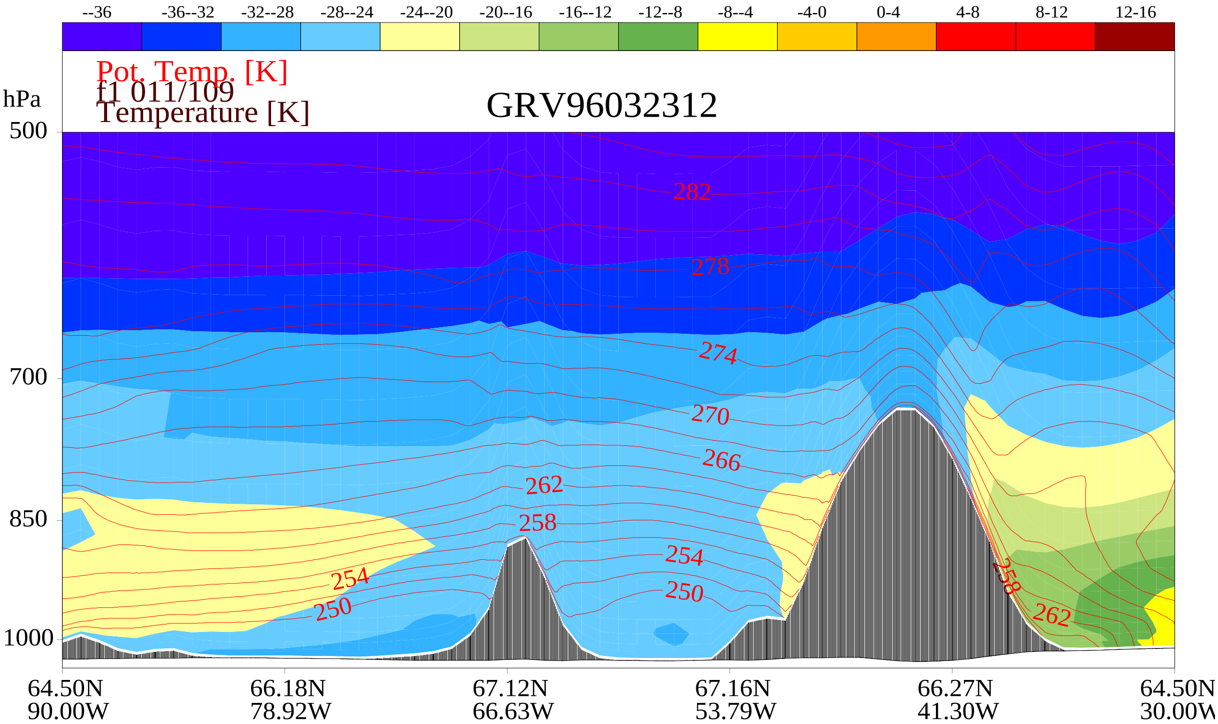

Fig. 16.a-b: Same as Fig. 13, but for the date 23.03.96 12 UTC.

DANISH METEOROLOGICAL INSTITUTE

Scientific Reports

Scientific reports from the Danish Meteorological Institute cover a variety of geophysical fields, i.e. meteorology (including climatology), oceanography, subjects on air and sea pollution, geomagnetism, solar-terrestrial physics, and physics of the middle and upper atmosphere.

Reports in the series within the last five years:

No. 94-1
Bjørn M. Knudsen: Dynamical processes in the ozone layer.

No. 94-2
J. K. Olesen and K. E. Jacobsen: On the atmospheric jet stream with clear air turbulences (CAT) and the possible relationship to other phenomena including HF radar echoes, electric fields and radio noise.

No. 94-3
Ole Bøssing Christensen and Bent Hansen Sass: A description of the DMI evaporation forecast project.

No. 94-4
I.S. Mikkelsen, B. Knudsen, E. Kyrö and M. Rummukainen: Tropospheric ozone over Finland and Greenland, 1988-94.

No. 94-5
Jens Hesselbjerg Christensen, Eigil Kaas, Leif Laursen: The contribution of the Danish Meteorological Institute (DMI) to the EPOCH project "The climate of the 21st century" No. EPOC-003-C (MB).

No. 95-1
Peter Stauning and T.J. Rosenberg: High-Latitude, Day-time Absorption Spike Events
1. Morphology and Occurrence Statistics.
Not Published.

No. 95-2
Niels Larsen: Modelling of changes in stratospheric ozone and other trace gases due to the emission changes : CEC Environment Program Contract No. EV5V-CT92-0079. Contribution to the final report.

No. 95-3
Niels Larsen, Bjørn Knudsen, Paul Eriksen, Ib Steen Mikkelsen, Signe Bech Andersen and Torben Stockflet Jørgensen: Investigations of ozone, aerosols, and clouds in the arctic stratosphere : CEC Environment Program Contract No. EV5V-CT92-0074. Contribution to the final report.

No. 95-4
Per Høeg and Stig Syndergaard: Study of the derivation of atmospheric properties using radio-occultation technique.

No. 95-5
Xiao-Ding Yu, **Xiang-Yu Huang** and **Leif Laursen** and Erik Rasmussen: Application of the HIRLAM system in China: Heavy rain forecast experiments in Yangtze River Region.

No. 95-6
Bent Hansen Sass: A numerical forecasting system for the prediction of slippery roads.

No. 95-7
Per Høeg: Proceeding of URSI International Conference, Working Group AFG1 Copenhagen, June 1995. Atmospheric Research and Applications Using Observations Based on the GPS/GLONASS System.

No. 95-8
Julie D. Pietrzak: A Comparison of Advection Schemes for Ocean Modelling.

No. 96-1
Poul Frich (co-ordinator), H. Alexandersson, J. Ashcroft, B. Dahlström, G.R. Demarée, A. Drebs, A.F.V. van Engelen, E.J. Førland, I. Hanssen-Bauer, R. Heino, T. Jónsson, K. Jonasson, L. Keegan, P.Ø. Nordli, **T. Schmith**, **P. Steffensen**, H. Tuomenvirta, O.E. Tveito: North Atlantic Climatological Dataset (NACD Version 1) - Final Report.

No. 96-2
Georg Kjærgaard Andreasen: Daily Response of High-latitude Current Systems to Solar Wind Variations: Application of Robust Multiple Regression. Methods on Godhavn magnetometer Data.

No. 96-3

Jacob Woge Nielsen, Karsten Bolding Kristensen, Lonny Hansen: Extreme sea level highs: A statistical tide gauge data study.

No. 96-4
Jens Hesselbjerg Christensen, Ole Bøssing Christensen, Philippe Lopez, Erik van Meijgaard, Michael Botzet: The HIRLAM4 Regional Atmospheric Climate Model.

No. 96-5
Xiang-Yu Huang: Horizontal Diffusion and Filtering in a Mesoscale Numerical Weather Prediction Model.

No. 96-6
Henrik Svensmark and Eigil Friis-Christensen: Variation of Cosmic Ray Flux and Global Cloud Coverage - A Missing Link in Solar-Climate Relationships.

No. 96-7
Jens Havskov Sørensen and Christian Ødum Jensen: A Computer System for the Management of Epidemiological Data and Prediction of Risk and Economic Consequences During Outbreaks of Foot-and-Mouth Disease. CEC AIR Programme. Contract No. AIR3 - CT92-0652.

No. 96-8
Jens Havskov Sørensen: Quasi-Automatic of Input for LINCOM and RIMPUFF, and Output Conversion. CEC AIR Programme. Contract No. AIR3 - CT92-0652.

No. 96-9
Rashpal S. Gill and Hans H. Valeur:
Evaluation of the radarsat imagery for the operational mapping of sea ice around Greenland.

No. 96-10
Jens Hesselbjerg Christensen, Bennert Machenhauer, Richard G. Jones, Christoph Schär, Paolo Michele Ruti, Manuel Castro and Guido Visconti:
Validation of present-day regional climate simulations over Europe: LAM simulations with observed boundary conditions.

No. 96-11
Niels Larsen, Bjørn Knudsen, Paul Eriksen, Ib Steen Mikkelsen, Signe Bech Andersen and Torben Stockflet Jørgensen: European Stratospheric Monitoring Stations in the Artic: An European contribution to the Network for Detection of Stratospheric Change (NDSC): CEC Environment Programme Contract EV5V-CT93-0333: DMI contribution to the final report.

No. 96-12
Niels Larsen: Effects of heterogeneous chemistry on the composition of the stratosphere: CEC Environment Programme Contract EV5V-CT93-0349: DMI contribution to the final report.

No. 97-1
E. Friis Christensen og C. Skøtt: Contributions from the International Science Team. The Ørsted Mission - A Pre-Launch Compendium.

No. 97-2
Alix Rasmussen, Sissi Kiilsholm, Jens Havskov Sørensen, Ib Steen Mikkelsen: Analysis of Tropospheric Ozone Measurements in Greenland: Contract No. EV5V-CT93-0318 (DG 12 DTEE): DMI's contribution to CEC Final Report Arctic Trophospheric Ozone Chemistry ARCTOC.

No. 97-3
Peter Thejll: A Search for Effects of External Events on Terrestrial Atmospheric Pressure: Cosmic Rays

No. 97-4
Peter Thejll: A Search for Effects of External Events on Terrestrial Atmospheric Pressure: Sector Boundary Crossings

No. 97-5
Knud Lassen: Twentieth Century Retreat of Sea-Ice in the Greenland Sea

No. 98-1
Niels Woetman Nielsen, Bjarne Amstrup, Jess U. Jørgensen:
HIRLAM 2.5 parallel tests at DMI:
Sensitivity to type of schemes for turbulence, moist processes and advection

No. 98-2
Per Høeg, Georg Bergeton Larsen, Hans-Henrik Benzon, Stig Syndergaard, Mette Dahl Mortensen:
The GPSOS project
Algorithm Functional Design and Analysis of ionosphere, Stratosphere and Troposphere Observations

No. 98-3
Dahl Mortensen, Mette; Per Høeg:
Satellite Atmosphere Profiling Retrieval in a Nonlinear Troposphere
Previously entitled: Limitations Induced by Multipath

No. 98-4

Dahl Mortensen, Mette Per Høeg:
Resolution Properties in Atmospheric Profiling with GPS

No. 98-5
Gill, R. S. and M. K. Rosengren
Evaluation of the Radarsat Imagery for the Operational Mapping of Sea Ice around Greenland in 1997.

No. 98-6
Gill, R. S., Valeur, H. H., Nielsen, P. and Hansen, K. Q.: Using ERS SAR images in the operational mapping of sea ice in the Greenland waters: final report for ESA-ESRIN's: pilot projekt no. PP2.PP2.DK2 and 2nd Announcement of opportunity for the exploitation of ERS data projekt No. AO2..DK 102.

No. 98-7
Høeg, Per et al.: GPS Atmosphere Profiling Methods and Error Assessments.

No. 98-8
Svensmark, H., N. Woetmann Nielsen and A.M. Sempreviva: Large Scale Soft and Hard Turbulent States of the Atmosphere.

No. 98-9
Lopez, Philippe, Eigil Kaas and Annette Guldberg: The Full Particle-In-Cell advection scheme in spherical geometry**.**

No. 98-10
Svensmark, H.: Influence of Cosmic Rays on Earth's Climate.

No. 98-11
Thejll, Peter and Henrik Svensmark: Notes on the method of normalized multivariate regression.

No. 98-12
Lassen. K: Extent of sea ice in the Greenland Sea 1977-1997: an extension of DMI Scientific Report 97-5

No. 98-13
Larsen, Niels; Adriani, Alberto and Donfrancesco, Guido Di: Microphysical analysis oof plar stratospheric clouds observed by Lidar at McMurco, Antarctica

No.98-14
Dahl Mortensen, Mette: The Back-Propagation Method for Inversion of Radio Occultation Data.